

## A DIFFERENTIAL EFFECT OF GRAPHENE OXIDE ON THE PRODUCTION OF PROINFLAMMATORY CYTOKINES BY MURINE MICROGLIA

Hui-Ting Chen, Hsin-Ying Wu, Chih-Hua Shih and Tong-Rong Jan\*

*Department and Graduate Institute of Veterinary Medicine  
School of Veterinary Medicine, National Taiwan University  
No. 1, Sec. 4, Roosevelt Road, Taipei 106, Taiwan, ROC*

Received 14 May 2015

Accepted 6 July 2015

Published 13 August 2015

### ABSTRACT

Graphene oxide (GO) is a promising nanomaterial for application in a variety of biomedical fields, including neuro-oncology, neuroimaging, neuroregeneration and drug delivery. Microglia are the central macrophage-like cells critically involved in neuroimmunity. However, the interaction between GO and microglia remained mostly unknown. The present study investigated the influence of GO on the production of proinflammatory cytokines by microglia. Primary murine microglial cells were treated with GO (1–25  $\mu\text{g}/\text{mL}$ ) followed by stimulation with lipopolysaccharide (LPS) for 24 h. The cell viability was measured by spectrophotometry using AlamarBlue®. The levels of interleukin (IL)-1 $\beta$  and tumor necrosis factor (TNF)- $\alpha$  in the supernatants were measured by enzyme-linked immunosorbent assay (ELISA). The IL-1 $\beta$  converting enzyme (ICE) activity was measured using a specific fluorescent substrate. The activity of cathepsin B and the lysosomal permeability and alkalinity were determined by flow cytometry. Treatment with GO did not affect cell viability, but significantly suppressed the production of IL-1 $\beta$ . In contrast, the production of TNF- $\alpha$  was unaltered. In addition, the lysosomal permeability and alkalinity in microglia treated with GO were increased, whereas the activity of cathepsin B and ICE was decreased. Collectively, these results demonstrated that exposure to GO differentially affected the production of proinflammatory cytokines, which is associated with the modulation of the lysosomal pathway of cytokines processing.

**Keywords:** Graphene oxide; Interleukin-1 $\beta$ ; Lipopolysaccharide; Lysosome; Microglia.

### INTRODUCTION

Graphene has attracted a lot of attention in recent years due to their unique electronic, mechanical, thermal and optical properties, which endow its promising

application in a wide spectrum of fields, including electronics and biomedicine.<sup>1,2</sup> In particular, graphene-based nanomaterials have been studied for neuroimaging, neuroregeneration, drug delivery and photothermal

\*Corresponding author: Tong-Rong Jan, Department and Graduate Institute of Veterinary Medicine, National Taiwan University, No. 1, Sec. 4, Roosevelt Road, Taipei 106, Taiwan, ROC. Tel: +886233661287; Fax: +886233663257; E-mail: tonyjan@ntu.edu.tw

brain cancer therapy.<sup>3–5</sup> Upon systemic administration, graphene-based nanomaterials have been found mainly accumulated in the liver and spleen.<sup>6–8</sup> Previous studies reported that graphene-based nanomaterials affected the viability and functionality of macrophages, including the induction of cell death, the suppression of phagocytic activity and the enhancement of proinflammatory cytokine production.<sup>9–14</sup> In light of the increasing applications of graphene-based nanomaterials in the fields of neurotherapeutics and neuroengineering, the interaction between brain cells and graphene is a relevant issue to be addressed. To date, it remains mostly elusive if graphene influences the functionality of microglia, the brain-resident macrophage-like immune cells.

Microglia are responsible for the surveillance of homeostasis in the central nervous system (CNS). In the mature brain, microglia typically exist in a resting state characterized by ramified morphology. Upon brain injury, foreign agent invasion and pathogen infection, microglia are rapidly activated, and undergo morphologic and functional alterations. Activated microglia produce proinflammatory cytokines and cytotoxic factors, including interleukin (IL)-1 $\beta$ , nitric oxide (NO), tumor necrosis factor (TNF)- $\alpha$  and reactive oxygen species (ROS). These mediators play a key role in the prevention of brain cells from further damage and to promote the repair of the damaged tissue.<sup>15,16</sup> Recently, it has been reported that gold, iron oxide, silica and titanium oxide nanoparticles influence the morphology and functionality of microglial cells.<sup>17–21</sup> However, evidence pertaining to the effects of graphene on the functionality of microglia remains scarce. The objective of this study was to investigate the effect of graphene oxide (GO) on the production of proinflammatory cytokines by activated microglia.

## MATERIALS AND METHODS

### Reagents and Chemicals

All reagents were purchased from Sigma Chemical (St. Louis, MO) unless otherwise stated. GO (thickness: 2 nm) was synthesized as previously described.<sup>22</sup> Dulbecco's Modified Eagle Medium (DMEM) was obtained from Caisson Laboratories (Rexburg, ID). Fetal bovine serum (FBS), horse serum (HS) and cell culture reagents were purchased from GIBCO BRL (Gaithersburg, MD). Enzyme-linked immunosorbent assay (ELISA) sets for cytokine measurement were purchased from BD Biosciences (San Diego, CA). IL-1 $\beta$  converting

enzyme (ICE)/Caspase-1 protease assay kit and fluorogenic substrates Ac-YVAD-AFC (7-amino-4-methylcoumarin) were obtained from Chemicon (Temecula, CA) and Tocris (Bristol, UK), respectively. Magic Red<sup>TM</sup> cathepsin B detection kit was purchased from Immunochemistry Technologies (Bloomington, MN).

### Particle Size Analysis of GO

The particle size distribution of GO in double distilled water (DDW) and in the cell-cultured medium DMEM was measured by dynamic light scattering using a particle size analyzer (Zetasizer Nano S, Malvern Instruments Ltd., Malvern, Worcestershire, UK).

### Culture of Primary Murine Microglial Cells

Primary microglia were prepared from cerebral cortices of 0–2 days old BALB/c mice (BioLasco, Ilan, Taiwan). After removing meninges aseptically, the brain cells were resuspended in DMEM containing 10% heat inactivated FBS, 10% HS, 4 mM L-glutamine, 100 U/mL penicillin and 100  $\mu$ g/mL streptomycin and cultured on the flasks coated with 25  $\mu$ g/mL poly-D-lysine. Upon reaching confluence (12–16 days), loosely adherent microglial cells were collected by shaking at 165 rpm at 37°C for 3 h. The enriched microglial cells were cultured on culture plates for 2 h to allow attachment, and then the medium was changed to DMEM containing 1% HS, 4 mM L-glutamine, 100 U/mL penicillin and 100  $\mu$ g/mL streptomycin for experiments with GO exposure. In all cases, the cells were cultured at 37°C in 5% CO<sub>2</sub>. The purity of microglial culture was >90% as determined by flow cytometry with CD 11b staining.

### Measurement of Cell Viability

The viability of microglia was determined by the AlamarBlue<sup>®</sup> assay. Microglial cells ( $4 \times 10^5$  cells/mL) were cultured in quadruplicate in opaque 96-well plates (0.1 mL/well). The cells were either left untreated (naïve; NA) or treated with GO (1–25  $\mu$ g/mL) and/or vehicle (VH; distilled water) for 30 min followed by stimulation with lipopolysaccharide (LPS; 100 ng/mL) for 24 h. An AlamarBlue<sup>®</sup> stock solution was added to each well (10  $\mu$ L/well) 4 h before the end of incubation. At the end of incubation, the fluorescence of reduced AlamarBlue<sup>®</sup> was measured using a microplate reader with excitation at 560 nm and emission at 590 nm (SpectraMax M5, Molecular Devices, Sunnyvale, CA).

## Cell Cultures for Cytokine Measurement

Microglial cells ( $4 \times 10^5$  cells/mL) were cultured in triplicate in 48-well plates (0.25 mL/well). The cells were either left untreated (naïve; NA) or treated with GO (1–25  $\mu\text{g/mL}$ ) and/or VH for 30 min followed by stimulation with LPS (100 ng/mL) for 24 h to induce appropriate levels of IL-1 $\beta$  and TNF- $\alpha$  in the supernatants allowing to be quantified by standard sandwich ELISA.

## Measurement of ICE Activity Using Enzymatic Assay

Microglial cells ( $4 \times 10^5$  cells/mL) were cultured in 6 cm dishes (5.5 mL/dish) and treated with GO and LPS as described above. After washing, the cells were harvested and lysed with cell lysis buffer. The lysates were incubated with 200  $\mu\text{M}$  of the ICE fluorogenic substrates Ac-YVAD-AFC and 5 mM of DTT for 2 h at 37°C, and the fluorescence was measured at 400 nm excitation and 505 nm emissions (SpectraMax M5, Molecular Devices, Sunnyvale, CA).

## Detection of Cathepsin B Enzyme Activity

Microglial cells ( $4 \times 10^5$  cells/mL) were cultured in triplicate in 48-well plates (0.25 mL/well) and treated with GO and LPS as described above. The cells were stained with Magic Red™ cathepsin B substrate for 1 h at 37°C. Once the substrate is cleaved by active cathepsin B, its product emits red fluorescence whose intensity is a direct measurement of the enzymatic activity of cathepsin B. After washing, the fluorescence of 5000 single cells for each sample was measured using a flow cytometer at emission of 610 nm (BD LSRFortessa cell analyzer, BD Biosciences, San Jose, CA). Data were analyzed using the software Flowjo7.5 (Tree Star Inc., Ashland, OR).

## Measurement of Lysosomal Acidity and Permeability

The acidity and permeability of lysosome were determined by flow cytometry using LysoSensor™ Green DND-189 and acridine orange, respectively. Microglial cells ( $4 \times 10^5$  cells/mL) were cultured in triplicate in 48-well plates (0.25 mL/well) and treated with GO and LPS as described above. The cells were stained with 1  $\mu\text{M}$  LysoSensor™ for 2 h or 5  $\mu\text{g/mL}$  acridine orange for 10 min at 37°C. After washing, the fluorescence of

5000 single cells for each sample was measured using a flow cytometer at emission of 525 nm and 610 nm for LysoSensor™ and acridine orange, respectively (BD LSRFortessa cell analyzer, BD Biosciences, San Jose, CA). Data were analyzed using the software Flowjo7.5 (Tree Star Inc., Ashland, OR).

## Statistical Analysis

The mean  $\pm$  standard error (SE) was determined for each treatment group in the individual experiments. Homogeneous data were evaluated by a parametric analysis of variance, and Dunnett's two-tailed *t*-test was used to compare treatment groups to the control group. \**p* < 0.05 was defined as statistical significance.

## RESULTS AND DISCUSSION

### Particle Size Analysis of GO

GO with the thickness of 2 nm was synthesized by a modified Hummers' method.<sup>23,24</sup> The particle size distribution of GO was measured by dynamic light scattering. The GO in distilled water exhibited two peaks of size distribution with average particle sizes of 11 nm and 179 nm. When the GO was diluted with cell-cultured medium (DMEM containing 1% HS), three peaks of size distribution with average particle sizes of 4, 13 and 126 nm were measured (Fig. 1).

### GO Did Not Affect the Viability of Primary Microglia

Previous studies demonstrated that graphene and GO induced cell death in immortalized and primary macrophages.<sup>9–12</sup> It is currently unclear whether GO

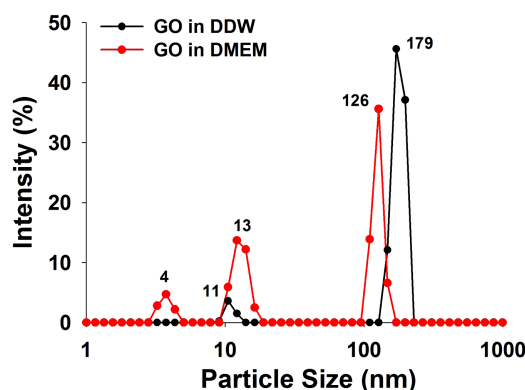


**Fig. 1** Particle size analysis of GO. The particle size distribution of GO in DDW and in the cell culture medium DMEM was measured by dynamic light scattering.

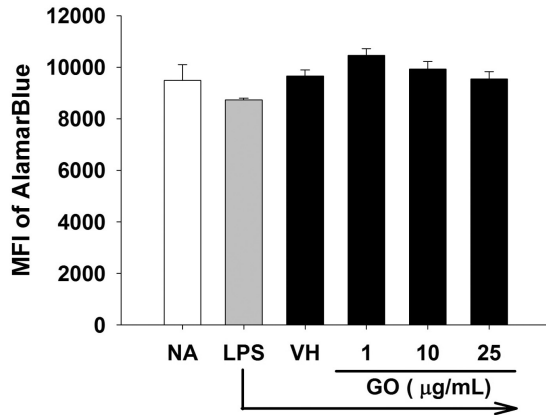


**Fig. 2** GO did not affect the viability of primary microglia. Microglia ( $4 \times 10^5$  cells/mL) were either left untreated (NA), or treated with VH ( $H_2O$ ) and/or GO (1–25  $\mu g/mL$ ) for 30 min, followed by stimulation with LPS (100 ng/mL) for 24 h. The cell viability was determined by the AlamarBlue® assay. Data are expressed as the mean  $\pm$  SE of quadruplicate cultures. Results are a representative of three independent experiments.

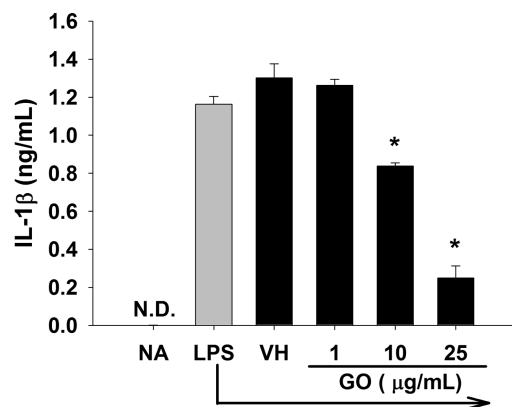
Note: MFI, mean fluorescence intensity.

affect the viability of primary microglia. Hence, we firstly measured the cell viability of microglial cells exposed to GO using the AlamarBlue® assay. Exposure of LPS-activated microglia to GO (1–25  $\mu g/mL$ ) for 24 h did not affect the mean fluorescence intensity of AlamarBlue®, as compared to the VH control (Fig. 2), indicating that the employed concentration range of GO did not affect the cell viability. The concentration range of GO was chosen according to previous reports showing cytotoxic effects of GO and graphene on macrophages.<sup>10,11</sup> Several factors might affect the cytotoxicity of GO, including the particle size, shape, surface modification and the condition and types of cells. As the size of GO used in the present study was less than 200 nm, which was far smaller than that (1–2  $\mu m$ ) of GO used in macrophages in previous studies,<sup>11</sup> suggesting that the size may be a key factor dictating the cytotoxicity of GO. Nonetheless, the difference between macrophages and microglia cannot be ruled out. Further studies are required to elucidate the relationship between particle size and cytotoxicity of GO in different phagocytes.

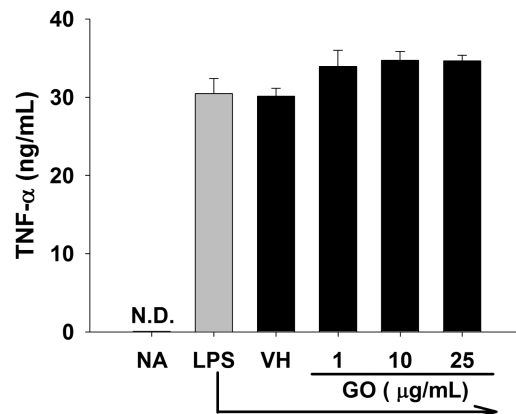
### GO Differentially Modulated the Production of Proinflammatory Cytokines by LPS-Stimulated Microglia

To address the potential impact of GO on the functionality of microglia, we examined the production of

proinflammatory cytokines by LPS-stimulated microglia. The concentration (100 ng/mL) of LPS was chosen according to previous reports showing the effective activation of microglia and the production of proinflammatory cytokines.<sup>21</sup> Exposure of LPS-activated microglia to GO significantly inhibited the production of IL-1 $\beta$ , but not TNF- $\alpha$  (Fig. 3). Previous studies showed that PEG-coating GO differentially regulated the production of proinflammatory cytokines in RAW264.7 macrophages, in which TNF- $\alpha$  was enhanced and IL-1 $\beta$  was unaltered.<sup>25</sup> Interestingly, our recent report demonstrated that iron oxide nanoparticles differentially



(A)



(B)

**Fig. 3** GO differentially modulated the production of proinflammatory cytokines by LPS-stimulated microglia. Microglia ( $4 \times 10^5$  cells/mL) were either left untreated (NA), or treated with VH ( $H_2O$ ) and/or GO (1–25  $\mu g/mL$ ) for 30 min, followed by stimulation with LPS (100 ng/mL) for 24 h. The level of (A) IL-1 $\beta$  and (B) TNF- $\alpha$  in the supernatants was measured by ELISA. Data are expressed as the mean  $\pm$  SE of triplicate cultures. Results are a representative of three independent experiments. \* $p < 0.05$  compared to the VH group.

Note: N.D., the level of cytokine is below the limit of quantification.

modulated the production of IL-1 $\beta$  and TNF- $\alpha$  in primary microglia, in which iron oxide nanoparticles accumulated in lysosomes, inhibited the secretory lysosomal pathway of IL-1 $\beta$  processing and thus suppressed the production of IL-1 $\beta$ .<sup>21</sup> By contrast, PEG-coating GO has been shown to localize with F-actin in RAW264.7 macrophages.<sup>25</sup> Collectively, these results suggested that the differential effects of nanoparticles on the production of proinflammatory cytokines in macrophages and microglia may be attributed to the different intracellular targets affected by nanoparticles.

### GO Attenuated the Activity of ICE and Secretory Lysosomal Cathepsin B in LPS-Activated Microglia

The maturation of IL-1 $\beta$  required the proteolytic cleavage of pro-IL-1 $\beta$  by the ICE (caspase-1).<sup>26</sup> In activated microglia, the secretory lysosomal enzyme cathepsin B has been shown to play a critical role in the processing and maturation of IL-1 $\beta$  through the activation of pro-caspase-1.<sup>21,27</sup> To elucidate the potential mechanisms contributing to the suppressive effect of GO on the production of IL-1 $\beta$  by activated microglia, the activity of ICE and cathepsin B was measured using specific fluorescent substrates. Consistent with the suppressive effect on IL-1 $\beta$  production, exposure to GO significantly attenuated the activity of ICE (Fig. 4(A)) and cathepsin B (Fig. 4(B)) in LPS-activated microglia. These results demonstrated that exposure to GO

inhibited the secretory lysosomal pathway of IL-1 $\beta$  processing and maturation in activated microglia, suggesting that lysosomes are a critical intracellular target for GO. This notion was supported by previous results showing the accumulation of GO in the lysosomes of murine macrophages.<sup>12</sup>

### GO Elevated Lysosomal Alkalinity and Permeability in LPS-Activated Microglia

Previous studies demonstrated that the accumulation of GO in lysosomes resulted in lysosomal dysfunction in murine macrophages.<sup>12</sup> Our results showed that GO inhibited the cathepsin B enzyme activity of lysosomes in activated microglia. Hence, we further investigated the potential impact of GO on the lysosomes of microglia. Most of lysosomal enzymes function optimally in the acid environment.<sup>28</sup> We examined whether GO altered the acidity of lysosomes in LPS-activated microglia. The acidity of lysosomes was measured by flow cytometry using LysoSensor Green DND-189, which emits green fluorescence in acidic organelles, such as lysosomes. The mean fluorescent intensity of LysoSensor was markedly attenuated in GO-treated cells (Fig. 5(A)), indicating an elevated alkalinity in lysosomes. It has been reported that disruption of lysosomal integrity contributed to the alkalization and dysfunction of lysosomes.<sup>29,30</sup> Therefore, we examined the permeability of lysosomes using acridine orange that

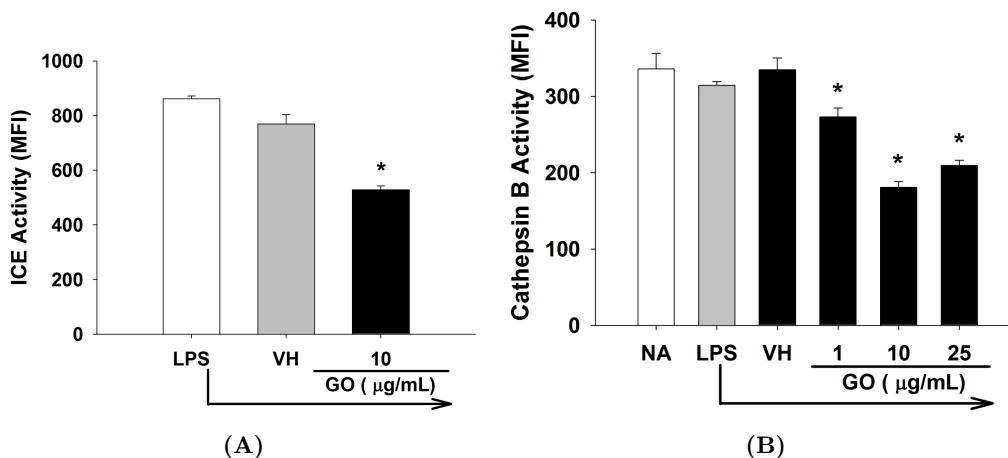


**Fig. 4** GO attenuated the activity of ICE and the cathepsin B enzyme activity of secretory lysosomes in LPS-activated microglia. Microglia were treated with VH ( $\text{H}_2\text{O}$ ) and/or GO (10  $\mu\text{g/mL}$ ) for 30 min, followed by stimulation with LPS (100 ng/mL) for 24 h. (A) The cell lysates were incubated with fluorogenic ICE substrates for 2 h at 37°C. The fluorescence of cleaved substrates was detected using a fluorescent microplate reader. (B) The cells were incubated with the cathepsin B substrate for 1 h at 37°C. The fluorescence of cathepsin B substrate was measured by flow cytometry. Data are expressed as the mean  $\pm$  SE of triplicate cultures. Results are a representative of two independent experiments. \* $p < 0.05$  compared to the VH group.



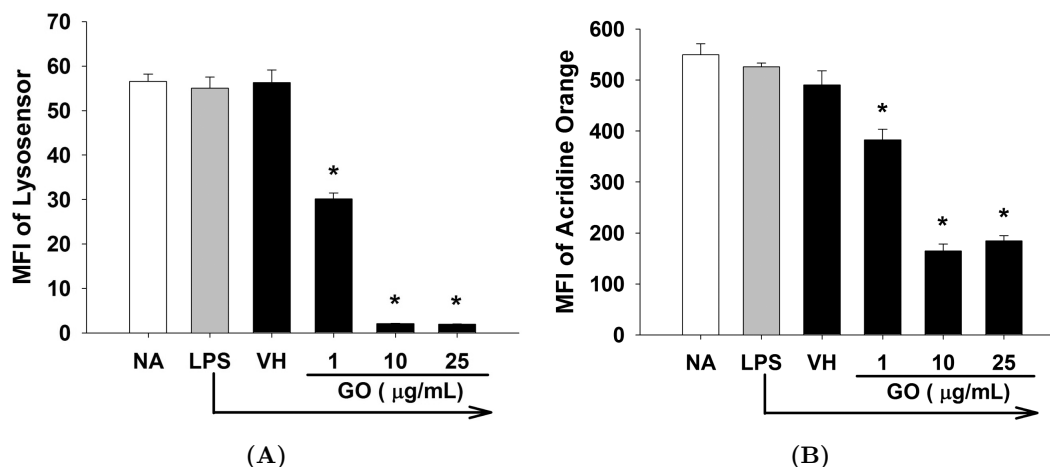


**Fig. 5** GO increased the alkalinity and permeability of lysosomes in LPS-activated microglia. Microglia were either left untreated (NA), or treated with VH ( $H_2O$ ) and/or GO (1–25  $\mu g/mL$ ) for 30 min, followed by stimulation with LPS (100 ng/mL) for 24 h. (A) The acidity and (B) permeability of lysosomes were measured by flow cytometry using LysoSensor Green and acridine orange, respectively. Data are expressed as the mean  $\pm$  SE of triplicate cultures. Results are a representative of two independent experiments. \* $p < 0.05$  compared to the VH group.

can be trapped in lysosomes and emits red fluorescence. Exposure of microglia to GO attenuated the fluorescent intensity of acridine orange (Fig. 5(B)), indicating an increased lysosomal permeability. Notably, the effects of GO at concentrations of 10  $\mu g/mL$  and 25  $\mu g/mL$  on the cathepsin B activity, and lysosomal acidity and permeability in microglia were comparable, implicating that GO at concentrations greater than 10  $\mu g/mL$  might reach a plateau effect on lysosomal functionality. Collectively, these results suggested that treatment with GO might impair lysosomal functions by elevating the lysosomal permeability and alkalinity in LPS-stimulated microglia. In addition, the disruption of lysosomal integrity may be a critical mechanism contributing to GO-mediated interruption of the secretory lysosomal processing of IL-1 $\beta$  production in LPS-activated microglia.

## CONCLUSION

The present study demonstrated a differential effect of GO on the production of proinflammatory cytokines by activated microglia, in which the suppression of IL-1 $\beta$  production was mediated by the inhibition of the secretory lysosomal processing pathway. These findings provide new insights to the potential impact of GO on the functionality of activated microglia and implied lysosomes as a crucial intracellular target for GO.

## ACKNOWLEDGMENTS

This work was supported in part by grant NSC103-2321-B002-008 from the Ministry of Science and Technology, Executive Yuan, Taiwan. Hui-Ting Chen and Hsin-Ying Wu contributed equally to this work.

## REFERENCES

- Allen MJ, Tung VC, Kaner RB, Honeycomb carbon: A review of graphene, *Chem Rev* **110**:132–145, 2010.
- Feng L, Liu Z, Graphene in biomedicine: Opportunities and challenges, *Nanomedicine (London)* **6**:317–324, 2011.
- Robinson JT, Tabakman SM, Liang Y, Wang H, Casalogue HS, Vinh D, Dai H, Ultrasmall reduced graphene oxide with high near-infrared absorbance for photothermal therapy, *J Am Chem Soc* **133**:6825–6831, 2011.
- Zhou K, Thouas GA, Bernard CC, Nisbet DR, Finkelstein DI, Li D, Forsythe JS, Method to impart electro- and biofunctionality to neural scaffolds using graphene-polyelectrolyte multilayers, *ACS Appl Mater Interfaces* **4**:4524–4531, 2012.
- Mattei TA, Rehman AA, Technological developments and future perspectives on graphene-based metamaterials: A primer for neurosurgeons, *Neurosurgery* **74**:499–516, 2014.
- Yang K, Gong H, Shi X, Wan J, Zhang Y, Liu Z, *In vivo* biodistribution and toxicology of functionalized nanographene oxide in mice after oral and intraperitoneal administration, *Biomaterials* **34**:2787–2795, 2013.
- Liu JH, Yang ST, Wang H, Chang Y, Cao A, Liu Y, Effect of size and dose on the biodistribution of graphene oxide in mice, *Nanomedicine (London)* **7**:1801–1812, 2012.

8. Yang K, Wan J, Zhang S, Zhang Y, Lee ST, Liu Z, *In vivo* pharmacokinetics, long-term biodistribution, and toxicology of PEGylated graphene in mice, *ACS Nano* **5**:516–522, 2011.
9. Chen GY, Yang HJ, Lu CH, Chao YC, Hwang SM, Chen CL, Lo KW, Sung LY, Luo WY, Tuan HY, Hu YC, Simultaneous induction of autophagy and toll-like receptor signaling pathways by graphene oxide, *Biomaterials* **33**:6559–6569, 2012.
10. Li Y, Liu Y, Fu Y, Wei T, Le Guyader L, Gao G, Liu RS, Chang YZ, Chen C, The triggering of apoptosis in macrophages by pristine graphene through the MAPK and TGF- $\beta$  signaling pathways, *Biomaterials* **33**:402–411, 2012.
11. Qu G, Liu S, Zhang S, Wang L, Wang X, Sun B, Yin N, Gao X, Xia T, Chen JJ, Jiang GB, Graphene oxide induces toll-like receptor 4 (TLR4)-dependent necrosis in macrophages, *ACS Nano* **7**:5732–5745, 2013.
12. Wan B, Wang ZX, Lv QY, Dong PX, Zhao LX, Yang Y, Guo LH, Single-walled carbon nanotubes and graphene oxides induce autophagosome accumulation and lysosome impairment in primarily cultured murine peritoneal macrophages, *Toxicol Lett* **221**:118–127, 2013.
13. Sasidharan A, Panchakarla LS, Sadanandan AR, Ashokan A, Chandran P, Girish CM, Menon D, Nair SV, Rao CN, Koyakutty M, Hemocompatibility and macrophage response of pristine and functionalized graphene, *Small* **8**:1251–1263, 2012.
14. Zhou H, Zhao K, Li W, Yang N, Liu Y, Chen C, Wei T, The interactions between pristine graphene and macrophages and the production of cytokines/chemokines via TLR- and NF- $\kappa$ B-related signaling pathways, *Biomaterials* **33**:6933–6942, 2012.
15. Aloisi F, Immune function of microglia, *Glia* **36**:165–179, 2001.
16. Kreutzberg GW, Microglia: A sensor for pathological events in the CNS, *Trends Neurosci* **19**:312–318, 1996.
17. Ma X, Wu Y, Jin S, Tian Y, Zhang X, Zhao Y, Yu L, Liang XJ, Gold nanoparticles induce autophagosome accumulation through size-dependent nanoparticle uptake and lysosome impairment, *ACS Nano* **5**:8629–8639, 2011.
18. Hutter E, Boridy S, Labrecque S, Lalancette-Hebert M, Kriz J, Winnik FM, Maysinger D, Microglial response to gold nanoparticles, *ACS Nano* **4**:2595–2606, 2010.
19. Choi J, Zheng Q, Katz HE, Guilarte TR, Silica-based nanoparticle uptake and cellular response by primary microglia, *Environ Health Perspect* **118**:589–595, 2010.
20. Long TC, Tajuba J, Sama P, Saleh N, Swartz C, Parker J, Hester S, Lowry GV, Veronesi B, Nanosize titanium dioxide stimulates reactive oxygen species in brain microglia and damages neurons *in vitro*, *Environ Health Perspect* **115**:1631–1637, 2007.
21. Wu HY, Chung MC, Wang CC, Huang CH, Liang HJ, Jan TR, Iron oxide nanoparticles suppress the production of IL-1 $\beta$  via the secretory lysosomal pathway in murine microglial cells, *Part Fibre Toxicol* **10**:46, 2013.
22. Wu HY, Lin KJ, Wang PY, Lin CW, Yang HW, Ma CC, Lu YJ, Jan TR, Polyethylene glycol-coated graphene oxide attenuates antigen-specific IgE production and enhanced antigen-induced T-cell reactivity in ovalbumin-sensitized BALB/c mice, *Int J Nanomed* **9**:4257–4266, 2014.
23. Yang HW, Lu YJ, Lin KJ, Hsu SC, Huang CY, She SH, Liu HL, Lin CW, Xiao MC, Wey SP, Chen PY, Yen TC, Wei KC, Ma CC, EGRF conjugated PEGylated nanographene oxide for targeted chemotherapy and photothermal therapy, *Biomaterials* **34**:7204–7214, 2013.
24. Yang HW, Hua MY, Hwang TL, Lin KJ, Huang CY, Tsai RY, Ma CC, Hsu PH, Wey SP, Hsu PW, Chen PY, Huang YC, Lu YJ, Yen TC, Feng LY, Lin CW, Liu HL, Wei KC, Non-invasive synergistic treatment of brain tumors by targeted chemotherapeutic delivery and amplified focused ultrasound-hyperthermia using magnetic nanographene oxide, *Adv Mater* **25**:3605–3611, 2013.
25. Feito MJ, Vila M, Matesanz MC, Linares J, Goncalves G, Marques PA, Vallet-Regi M, Rojo JM, Portoles MT, *In vitro* evaluation of graphene oxide nanosheets on immune function, *J Colloid Interface Sci* **432**:221–228, 2014.
26. Chauvet N, Palin K, Verrier D, Poole S, Dantzer R, Lestage J, Rat microglial cells secrete predominantly the precursor of interleukin-1 $\beta$  in response to lipopolysaccharide, *Eur J Neurosci* **14**:609–617, 2001.
27. Terada K, Yamada J, Hayashi Y, Wu Z, Uchiyama Y, Peters C, Nakanishi H, Involvement of cathepsin B in the processing and secretion of interleukin-1 $\beta$  in chromogranin A-stimulated microglia, *Glia* **58**:114–124, 2010.
28. Trombetta ES, Ebersold M, Garrett W, Pypaert M, Mellman I, Activation of lysosomal function during dendritic cell maturation, *Science* **299**:1400–1403, 2003.
29. Nilsson C, Johansson U, Johansson AC, Kagedal K, Ollinger K, Cytosolic acidification and lysosomal alkalization during TNF- $\alpha$  induced apoptosis in U937 cells, *Apoptosis* **11**:1149–1159, 2006.
30. Johansson AC, Appelqvist H, Nilsson C, Kagedal K, Roberg K, Ollinger K, Regulation of apoptosis-associated lysosomal membrane permeabilization, *Apoptosis* **15**:527–540, 2010.